iScience

CellPress
OPEN ACCESS

Article

ARID1A loss in pancreas leads to islet developmental defect and metabolic disturbance

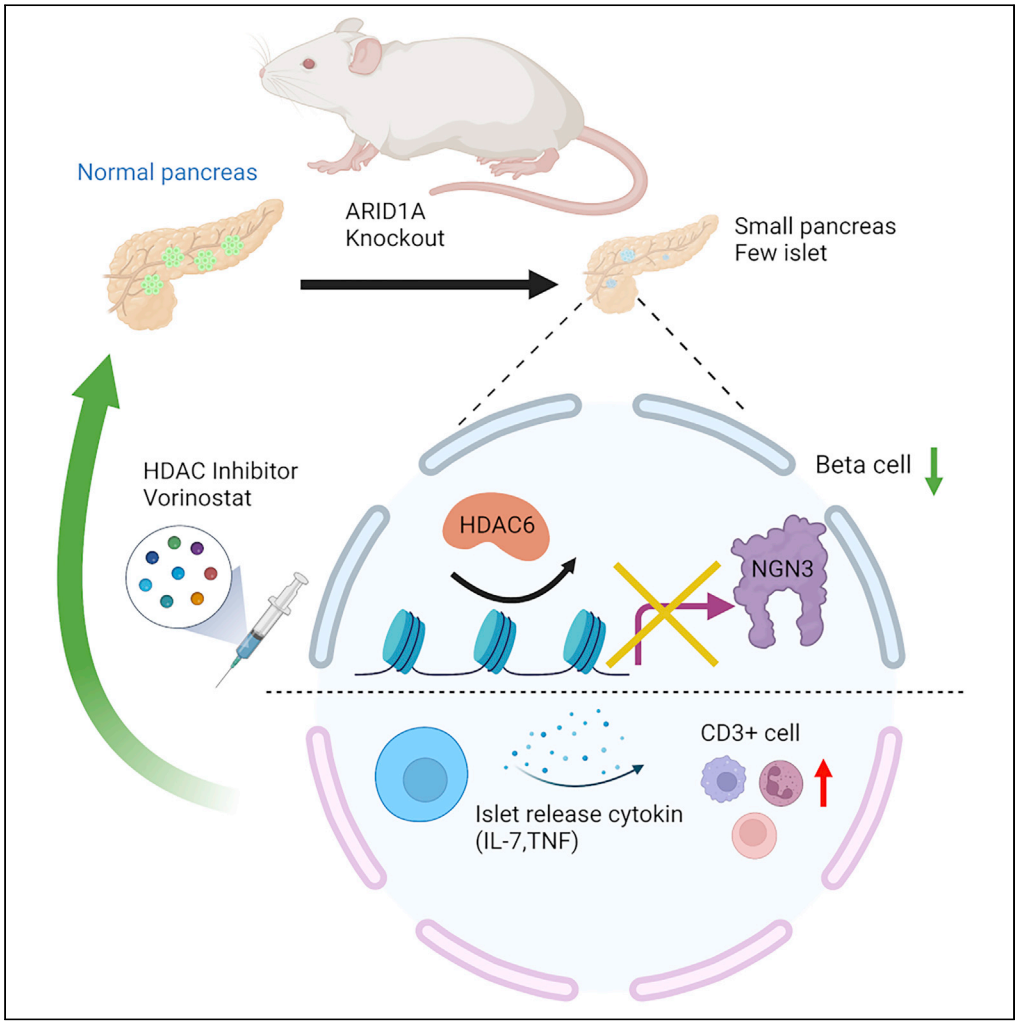

Tzu-Lei Kuo, Kuang-Hung Cheng, Li-Tzong Chen, Wen-Chun Hung

hung1228@nhri.edu.tw

Highlights

Depletion of Arid1a in the pancreas leads to islet defect and diabetes phenotype

Neurogenin 3 is a downstream mediator of Arid1a to control islet development

Expression of histone deacetylases is increased after Arid1a loss

Arid1a depletion alters genome-wide occupancy of histone deacetylase 6

Kuo et al., iScience *26*, 105881
January 20, 2023
https://doi.org/10.1016/j.isci.2022.105881

iScience

CellPress
OPEN ACCESS

Article

ARID1A loss in pancreas leads to islet developmental defect and metabolic disturbance

Tzu-Lei Kuo,[1] Kuang-Hung Cheng,[2] Li-Tzong Chen,[1,3,5] and Wen-Chun Hung[1,4,5,6,*]

SUMMARY

***ARID1A* is a tumor suppressor gene mutated in 7–10% of pancreatic cancer patients. However, its function in pancreas development and endocrine regulation is unclear. We generated mice that lack *Arid1a* expression in the pancreas. Our results showed that deletion of the *Arid1a* gene in mice caused a reduction in islet numbers and insulin production, both of which are associated with diabetes mellitus (DM) phenotype. RNA sequencing of isolated islets confirmed DM gene signature and decrease of developmental lineage genes. We identified neurogenin3, a transcription factor that controls endocrine fate specification, is a direct target of Aird1a. Gene set enrichment analysis indicated the enhancement of histone deacetylase (HDAC) pathway after Arid1a depletion and a clinically approved HDAC inhibitor showed therapeutic benefit by suppressing disease onset. Our data suggest that Arid1a is required for the development of pancreatic islets by regulating Ngn3^{+}-mediated transcriptional program and is important in maintaining endocrine function.**

INTRODUCTION

Gene transcription in mammalian cells is tightly orchestrated by the recruitment of transcription factors, co-regulators, mediators, transcription initiation factors and RNA polymerase II to the promoter regions.[1,2] ATP-dependent chromatin remodeling complexes are co-regulators that alter chromatin configuration to promote the binding of transcription factors to DNA. This process initiates gene transcription as well as DNA replication and repair.[3,4]

There are four major families of ATP-dependent chromatin remodeling complexes in mammals, including the BAF complex. Mutations in the subunits of the BAF complex are found in >20% of human cancers.[5,6] The BAF complex evolved from the yeast SWItch and sucrose nonfermenting (SWI/SNF) complex. Of the BAF complex components, the AT-rich interactive domain-containing protein 1A (*ARID1A*) is the most commonly mutated subunit.[7] In addition, loss of ARID1A expression is associated with poor clinical outcome in various cancers.[8–10] To clarify the role of *Arid1a* in pancreatic tumorigenesis, recent studies generated *Arid1a*-deficient mice and combined a *k-ras* mutation with a *p53* deletion.[11–13] These studies concluded that Arid1a maintains acinar cell homeostasis and ductal cell differentiation, and that loss of Arid1a induces intraductal papillary mucinous neoplasms (IPMNs) in mice. The combination of *k-ras* and *p53* dysregulation accelerates the formation of pancreatic cancer from IPMNs. These data suggested that *Arid1a* functions as a tumor suppressor gene in pancreatic cancer. All of these studies used Ptf1a-driven Cre recombinase to deplete *Arid1a* gene in various cell types in the pancreas. However, Cre activity is extremely low or undetectable in the islet cells of Ptf1a-Cre mice.[14,15] In line with the finding, all three studies showed that the expression of Arid1a is retained in the islets of the mice.[11–13] Thus, whether Arid1a plays a role in islet development and endocrine regulation is still unknown.

Because conventional knockout of the *Arid1a* gene in mice caused embryonic lethality,[16] the involvement of *Arid1a* in organ development and functional regulation is also largely unclear at present. A recent study demonstrated that liver-specific deletion of *Arid1a* induced non-alcoholic steatohepatitis by modulating the genes that control hepatic lipogenesis and fatty acid oxidation via epigenetic regulation.[17] By using the pancreatic and duodenal homeobox 1 (Pdx1)-Cre mouse model, we demonstrate that Arid1a is required for the development of islets in mice and is a key player in controlling the functionality of pancreatic β cells.

[1]National Institute of Cancer Research, National Health Research Institutes, Tainan 704, Taiwan

[2]Institute of Biomedical Sciences, National Sun Yat-Sen University, Kaohsiung 804, Taiwan

[3]Division of Internal Medicine, College of Medicine, Kaohsiung Medical University, Kaohsiung 807, Taiwan

[4]School of Pharmacy, College of Pharmacy, Kaohsiung Medical University, Kaohsiung 807, Taiwan

[5]Department of Medical Research, Kaohsiung Medical University Hospital, Kaohsiung 807, Taiwan

[6]Lead contact

*Correspondence: hung1228@nhri.edu.tw

https://doi.org/10.1016/j.isci.2022.105881

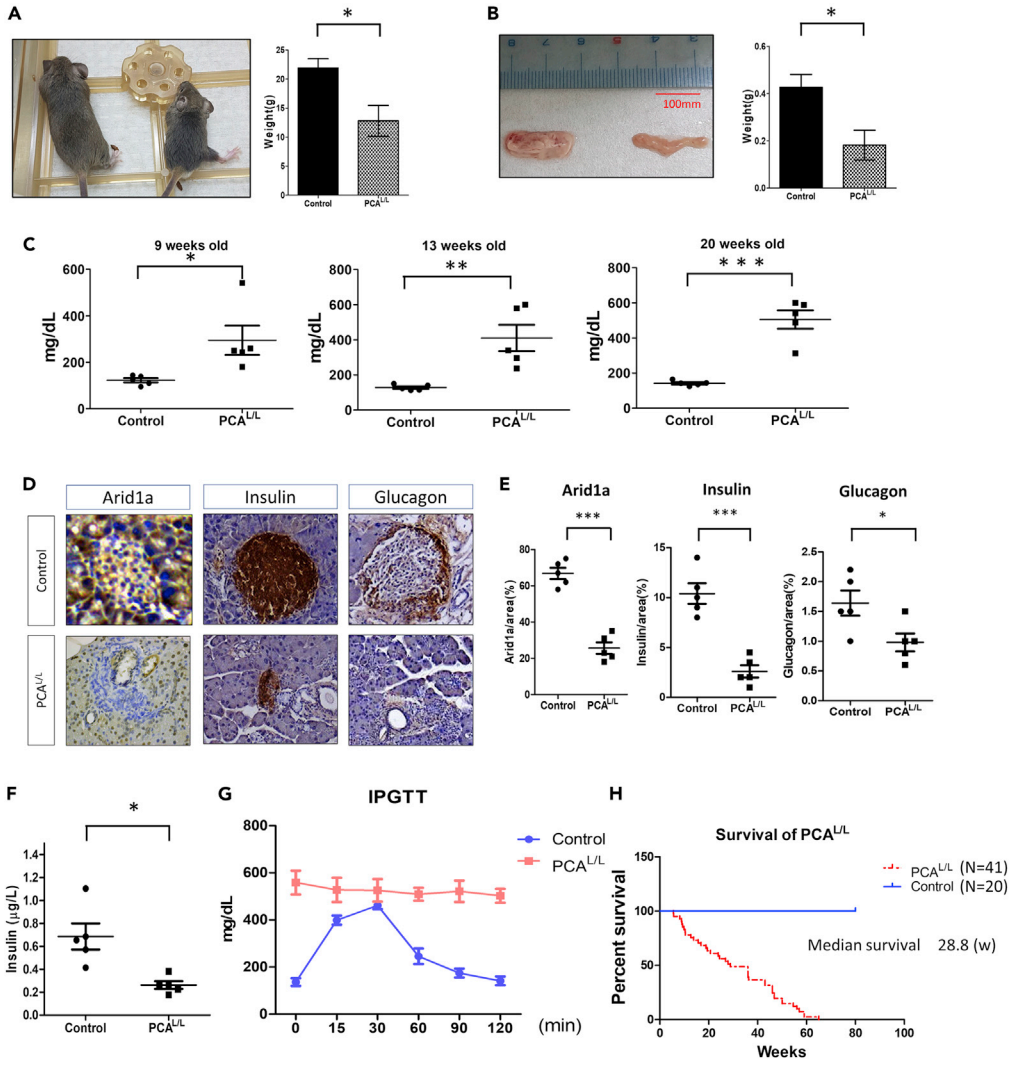

Figure 1. Pancreas-specific deletion of Arid1a induces DM in mice

(A) Body weight was decreased in the Arid1a-depleted PCA$^{L/L}$ mice (n = 5).

(B) The pancreas size of the PCA$^{L/L}$ mice was reduced (n = 5).

(C) Age-dependent increase of blood sugar in the Arid1a-depleted PCA$^{L/L}$ mice (n = 5).

(D) Representative pictures of Arid1a, insulin and glucagon staining in the pancreases of normal and Arid1a-depleted PCA$^{L/L}$ mice.

(E) The Arid1a-, insulin- and glucagon-positive areas were expressed as the percentage of total areas measured. Five independent areas were examined in a tissue slide and five tissues were counted in each group.

(F) Blood samples were collected from 13-week-old mice and insulin level was measured by ELISA assays. (n = 5).

(G) Thirteen-week-old mice (n = 5) were fasted for 6 h in the morning and intraperitoneally injected with 2 g/kg of glucose. Blood glucose levels were continuously measured for 120 min using a glucometer.

(H) The survival of control (n = 20) and PCA$^{L/L}$ mice (n = 41). *p<0.05; **p<0.01; ***p<0.001.

RESULTS

Deletion of Arid1a causes DM phenotype in mice

Pdx1 is a master regulator in the developing pancreas and is important for the maturation of β cells. We utilized Pdx1-Cre mice (PC mice) to perform a genetic cross with Arid1a$^{flox/flox}$ (A) mice to generate PCA$^{L/L}$ mice that lack *Arid1a* expression in the pancreas. *Arid1a* depletion was achieved by deleting the eighth exon of the *Arid1a* allele in the presence of Cre recombinase activity.[16] The PCA$^{L/L}$ mice were both viable and fertile; however, their body weight was decreased (Figure 1A). Pancreas size in the PCA$^{L/L}$ mice was significantly reduced (Figure 1B). We found that blood sugar levels were much higher

in the PCA$^{L/L}$ mice, and the magnitude of this difference increased with age (Figure 1C). Immunohistochemical (IHC) staining confirmed that Arid1a was absent in islet cells and was also reduced in acinar and ductal cells (Figure 1D). The morphology of acinar cells and the expression of amylase were not significantly changed (Figures S1A and S1B). Examination of liver, duodenum, prostate and pituitary gland did not find significant pathological alterations in these organs (Figure S2). However, the number and size of insulin-positive islets were significantly decreased in the pancreas of the PCA$^{L/L}$ mice (Figure 1E). The number of glucagon-expressing cells was also decreased (Figures 1D and 1E). In line with this finding, insulin levels in the blood were significantly reduced in the PCA$^{L/L}$ mice (Figure 1F). Glucose tolerance tests showed that blood sugar levels were much higher in the PCA$^{L/L}$ mice and did not decrease at 2 h following glucose challenge (Figure 1G). Blood chemistry analyses demonstrated significant alterations in liver and kidney functions and lipid metabolism (Figure S3). Total cholesterol and triacylglycerol were dramatically increased whereas total bilirubin and albumin were unchanged. Diabetic retinopathy, characterized by the thinning of inner plexiform and inner nuclear layers (Figures S4A and S4B), and thickening of the basement membrane of the vascular capillary (Figure S4C), was observed in the retinas of the aged (>20 weeks) PCA$^{L/L}$ mice. These results suggested that deletion of *Arid1a* impairs pancreas development and causes DM phenotype in mice. The survival of the PCA$^{L/L}$ mice was poor, with a median survival time of 28.8 weeks (Figure 1H). The clinical relevance of Arid1a expression in human DM was studied using the Human Pancreas Analysis Program Database (https://hpap.pmacs.upenn.edu), which was recently published.[18] Single-cell transcriptome analysis showed a 50% reduction of *ARID1A* expression in the islet cells of patients with DM, when compared with that of normal individuals (Figure S5A). We also extracted the microarray data from the dataset (GSE106148) reported previously.[19] Downregulation of *ARID1A*, detected by four independent probes, was found in the pancreases of DM patients (Figure S5B). These data support that *ARID1A* depletion may lead to pancreas dysfunction.

Arid1a depletion decreases insulin expression and increases MHC expression in mouse islet cells

Islets from the control and PCA$^{L/L}$ mice were isolated and compared. The morphology of the islets in culture was strikingly different, and the islet size of the PCA$^{L/L}$ mice was much smaller (Figure 2A). The insulin levels in the conditioned medium of cultured PCA$^{L/L}$ islets were significantly reduced (Figure 2B). RNA sequencing identified 4,048 differentially expressed genes (DEGs) with 3,040 upregulated after *Arid1a* depletion (Figure 2C). KEGG pathway analysis revealed several significantly altered pathways including pancreatic secretion, insulin secretion and DM phenotype (Figure 2D). Upregulations of MHC-I and MHC-II related genes were found in the DM gene signature in the *Arid1a*-depleted islets and were further confirmed by RT-PCR analysis (Figure S6). Gene set enrichment analysis (GSEA) also showed the downregulation of hallmark of pancreatic β cells and reduced expression of insulin, glucokinase (GCK) and glucose-6-phosphatase catalytic subunit 2 (G6PC2), three β cell-enriched genes (Figure 2E and Table S1). DM has been found to be associated with the upregulation of inflammatory cytokines.[20] Consistently, GSEA also demonstrated the activation of interferon α signaling (Figure 2F), which has been strongly implicated in DM.[21] In addition, we also found the upregulation of interleukin-1 β (IL-1β), another important inflammatory cytokine, in the *Arid1a*-depleted pancreas (Figure S7). Previous studies demonstrated that MHC-I and MHC-II are upregulated in the islets of DM patients.[22,23] Enhancements of several biological processes in KEGG analysis including leukocyte migration, regulation of defense response and T cell activation were all associated with enhanced immune reaction (Figure S8). Increase of a number of cytokines and chemokines in the isolated *Arid1a*-depleted islets was confirmed by RT-PCR analysis (Figure 2G). When examining the pancreatic tissues of the PCA$^{L/L}$ mice, a dramatic increase of T cell infiltration was observed (Figure 2H). Thus, pancreas-specific depletion of *Arid1a* in mice induces β cell dysfunction and triggers inflammation and immune attack in the pancreas that recapitulates the pathological alterations found in human DM.

Altered metabolism in Arid1a-depleted islet cells

In lung, Arid1a-deficiency leads to enhanced glycolysis pathway by enhancing transcription of PGAM1, PKM2, and PGK1.[24] In liver, Arid1a depletion impairs fatty acid oxidation by downregulating PPARα.[25] These studies suggested that a lack of Arid1a changes cell metabolism. To explore the cellular metabolic changes in islet cells under*Arid1a*-knockout condition, we isolated the islet cells from normal and PCA$^{L/L}$ mice and performed a comprehensive metabolomic analysis by capillary electrophoresis time-of-flight mass spectrometry. Principal component analysis revealed significant differences in metabolic pathways between the control and PCA$^{L/L}$ islet cells (Figure 3A). Differentially expressed metabolites were displayed by heatmap (Figure 3B). Top ten upregulated or downregulated metabolites were shown (Figures 3C and

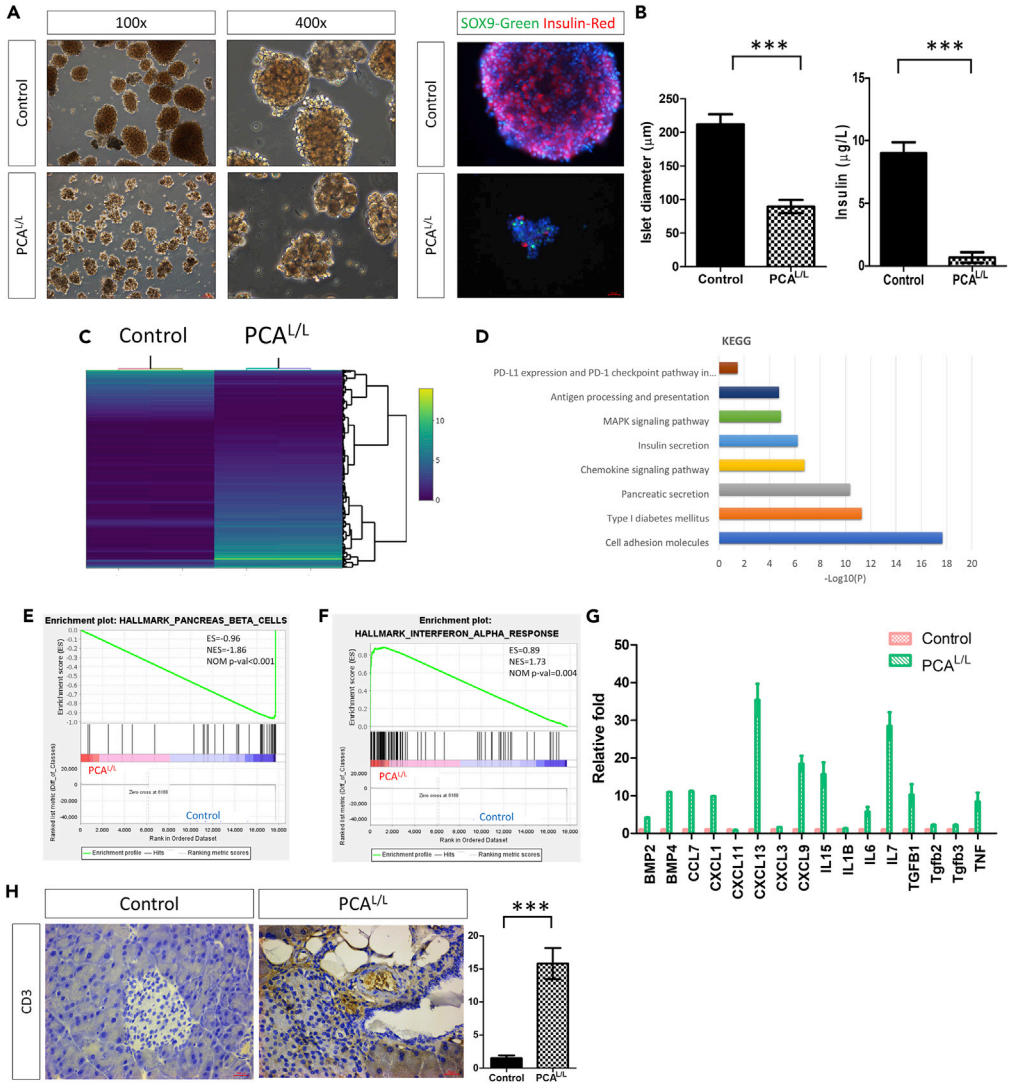

Figure 2. Arid1a depletion impairs islet development

(A) Islet isolation was performed as described in Materials and Methods. The cultured islets were imaged by light microscope and the islet size was calculated. The average diameters of the islets were expressed as Mean ± SD (n = 20).

(B) The conditioned media of control and isolated PCA$^{L/L}$ islets were collected at 72 h after culture and the levels of insulin were measured by ELISA assays.

(C) Gene expression of isolated control and PCA$^{L/L}$ islets was investigated by RNA sequencing and the expression profile was presented by heatmap.

(D) The pathways enriched in the PCA$^{L/L}$ islets studied by KEGG pathway analysis.

(E) GSEA analysis suggested β cell dysfunction in the isolated PCA$^{L/L}$ islets.

(F) Activation of interferon α signaling was found in the PCA$^{L/L}$ islets.

(G) Total RNAs were extracted from the isolated islets and the expression of cytokines and chemokines was studied by RT-PCR analysis.

(H) Pancreatic tissues collected from the control and PCA$^{L/L}$ mice. Infiltration of T cells in the pancreas was studied by IHC staining. (n = 5). ***p<0.001.

3D). The metabolite with the greatest increase was 2-oxoisovaleric acid, an intermediate highly upregulated in streptozotocin-induced DM.[26] In addition, elevated levels of 2-oxoglutaraic acid, pyruvic acid, glyceraldehyde-3-phosphate, lactic acid, and 3-hydroxybutyrate (a ketone body) were found in the PCA$^{L/L}$ islets, consistent with a diabetic phenotype (Figure 3E). Several amino acids including asparagine, aspartate, glutamate and alanine were also enhanced (Figure 3F). Of interest, N^1-methylnicotiamide, a metabolite that has been reported to be upregulated in the serum of DM patients,[27] was significantly elevated

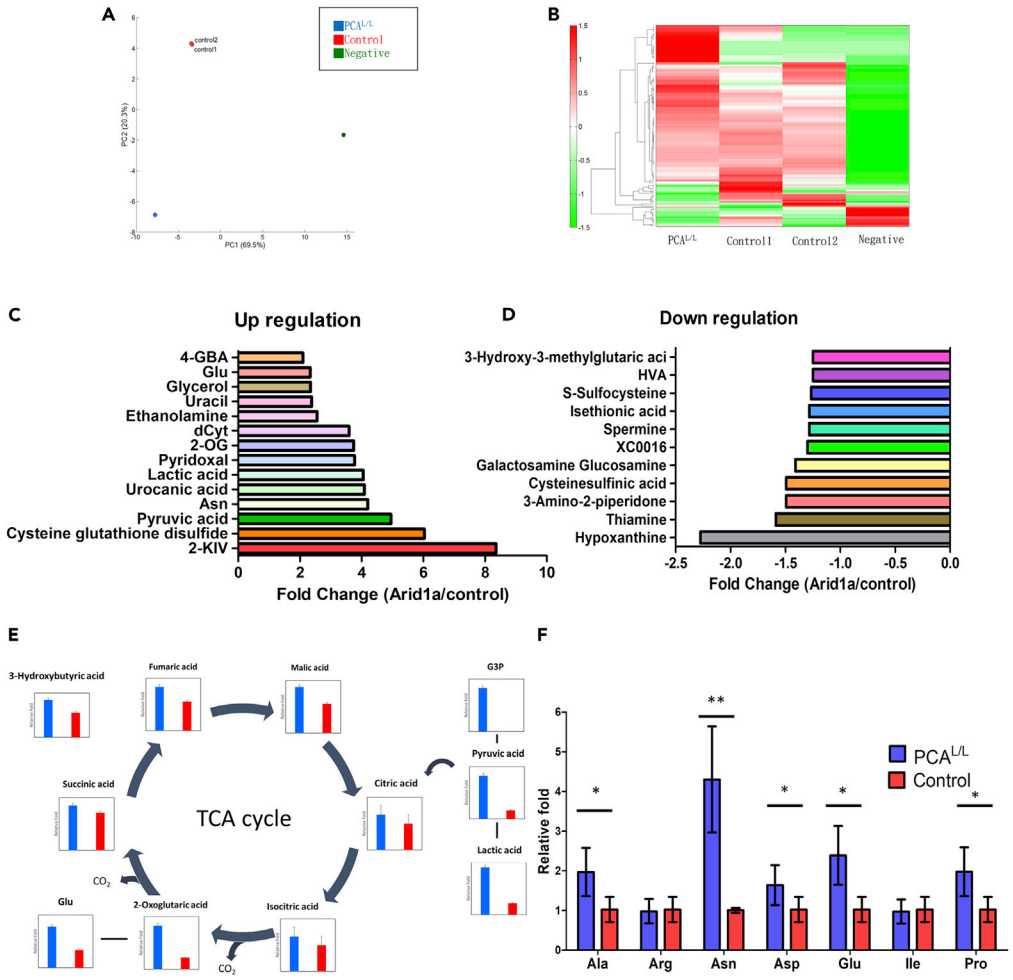

Figure 3. Metabolic alteration in the islets of the PCA$^{L/L}$ mice

(A) The metabolite profiles of the islets isolated from the control and PCA$^{L/L}$ mice were compared by principal component analysis.

(B) Differentially expressed metabolites were demonstrated by heatmap.

(C) Top 10 upregulated metabolites in the isolated PCA$^{L/L}$ islets were shown as fold change (Arid1a/control).

(D) Top 10 downregulated metabolites in the isolated PCA$^{L/L}$ islets were shown as fold change (Arid1a/control).

(E) Alteration of carbohydrate metabolism and increase of glycolytic intermediates in the isolated PCA$^{L/L}$ islets. The metabolite levels in the control islets (red color) and PCA$^{L/L}$ islets (blue color) were presented.

(F) The levels of various amino acids in the control islets (red color) and PCA$^{L/L}$ islets (blue color) were shown and the increase of alanine, aspartic acid, asparagine, glutamate, proline was found. *p<0.05; **p<0.01.

(Figure S9A). Other altered pathways included those involved in the biosynthesis of polyamine, purine and pyrimidine (Figure S9B). These results suggest that Arid1a depletion alters metabolism in the islet cells.

Developmental defect following Arid1a depletion

Significant reductions in body weight, pancreas size and islet number were found early in some mice at 5–6 weeks after birth. In addition, a number of transcription factors enriched in β cells were decreased in the *Arid1a*-depleted islets (Table S1). We tested whether Arid1a affects pancreas development. RT-PCR assays confirmed the data of RNA sequencing and demonstrated the downregulation of developmental lineage markers including *Pdx1* (a key regulator of pancreatic-specified endoderm development), *Hnf1B* (a crucial transcription factor in multipotent progenitors) and neurogenin 3 (*Ngn3*, a master controller of endocrine fate specification) in the *Arid1a*-depleted islets (Figure 4A). Because Ngn3 is a key transcription factor involved in the generation of endocrine progenitor cells, we studied whether *Ngn3* is a direct target gene of Arid1a. Bioinformatics analyses predicted four potential Arid1a binding sites in the *Ngn3* promoter (Figure 4B). Chromatin immunoprecipitation (ChIP) assays revealed

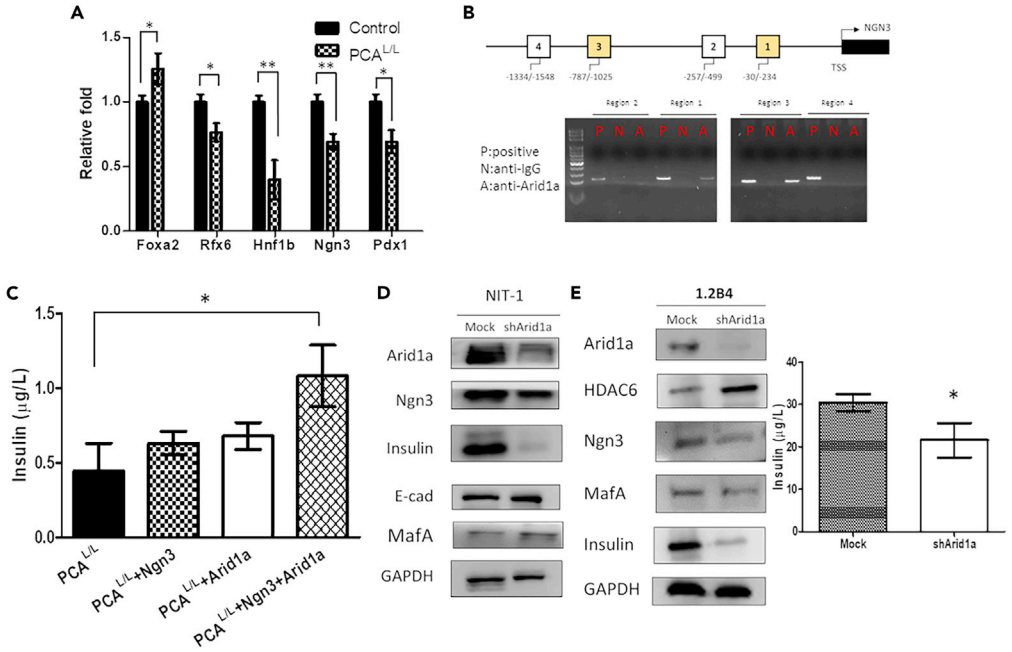

Figure 4. Ngn3 is a direct target of Arid1a

(A) The islets were collected from the control and PCA$^{L/L}$ mice and the expression of endocrine developmental lineage genes was studied by RT-PCR. *p<0.05; **p<0.01.

(B) Genomic DNAs were collected from the control and PCA$^{L/L}$ islets and ChIP assay was performed to study the binding of Arid1a to the predicted regions (marked from region 1 to 4 upstream of the transcriptional start site) in the Ngn3 gene promoter.

(C) Arid1a-depleted islet cells were infected with control (left) or Ngn3+Arid1a viral expression vectors. After 48 h, the conditioned media were collected and the insulin levels were determined by ELISA assay. (n = 5). *p<0.05.

(D) Mouse NIT-1 insulinoma cells were transfected with Arid1a shRNA and the protein levels of Arid1a, insulin and Ngn3 were analyzed by Western blotting. The expression levels of E-cadherin (E-Cad) and MafA were also examined.

(E) Human 1.2B4 insulin-secreting hybrid cells were transfected with Arid1a shRNA and the protein levels of ARID1A, Insulin and NGN3 were analyzed by Western blotting. The expression levels of HDAC6 and MafA were also examined. The insulin level in the conditioned media of cells transfected with control or shArid1a was determined by ELISA assay. (n = 3). *p<0.05.

the binding of Arid1a to two upstream regions of the *Ngn3* gene in the control islet cells but not in the *Arid1a*-depleted islet cells and the region 3 (Ngn3-3) was the major binding site of Arid1a in the *Ngn3* promoter (Figure 4B). We next performed rescue assay by expressing *Arid1a* and *Ngn3* in the isolated mouse islet cells (Figure 4C). Our results showed that expression of *Ngn3* alone could not significantly enhance insulin expression because of the lack of the SWI/SNF complex to appropriately remodeling the chromatin in the *Arid1a*-depleted islet cells. In addition, expression of *Arid1a* alone also could not fully activate insulin expression because the transfection efficiency of primarily isolated islet cells was very low (around 10%) and could not effectively trigger *Ngn3* expression in these cells. However, co-expression of *Ngn3* and *Arid1a* indeed upregulated insulin levels by three-fold in *Arid1a*-depleted islet cells (Figure 4C). Of interest, we found that mouse NIT-1 insulinoma cells expressed high levels of Arid1a and knockdown of Arid1a by shRNA decreased *Ngn3* and insulin expression (Figure 4D). We next used human 1.2B4 cell line, an insulin-secreting hybrid cell line generated by electrofusion of a primary culture of human pancreatic islets with HuP-T3 human pancreatic carcinoma cells, to verify our finding. Knockdown of *ARID1A* also reduced the expression of Ngn3 and insulin in 1.2B4 cells, accompanying with decreased insulin level in the cultured medium (Figure 4E). These results suggest that *Arid1a* depletion leads to developmental defect of β cells, and Ngn3 is one of the downstream targets for Arid1a to control β cell differentiation and maturation.

Upregulation of histone deacetylases (HDACs) in *Arid1a*-depleted pancreas

An enriched gene signature in our RNA sequencing data is the HDAC pathway (Figure 5A). We found the expressions of HDAC4, 5 and 6 were upregulated whereas the expression of HDAC1 was reduced in *Arid1a*-depleted pancreas tissues (Figure 5B). In agreement with this data, HDAC6 expression was

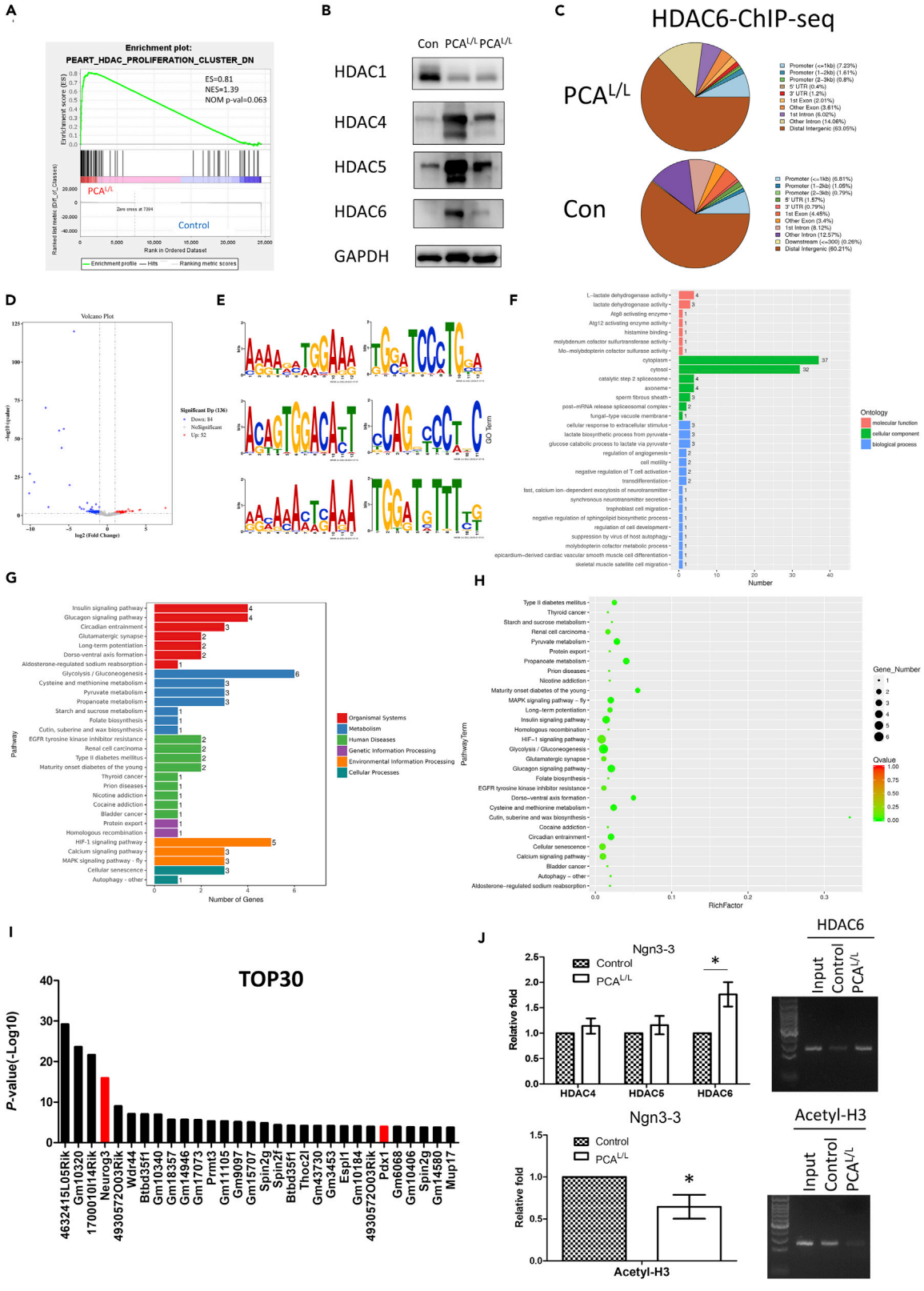
A
Enrichment plot:
PEART_HDAC_PROLIFERATION_CLUSTER_DN
ES=0.81
NES=1.39
NOM p-val=0.063
PCA^L/L
Control
Rank in Ordered Dataset
B
Con PCA^L/L PCA^L/L
HDAC1
HDAC4
HDAC5
HDAC6
GAPDH
C
HDAC6-ChIP-seq
PCA^L/L
Con
D
Volcano Plot
E
F
Ontology
molecular function
cellular component
biological process
Number
G
Pathway
Number of Genes
Organismal Systems
Metabolism
Human Diseases
Genetic Information Processing
Environmental Information Processing
Cellular Processes
H
PathwayTerm
RichFactor
Gene_Number
Qvalue
I
TOP30
P-value(-Log10)
J
Ngn3-3
Control
PCA^L/L
Relative fold
HDAC4
HDAC5
HDAC6
HDAC6
Input
Control
PCA^L/L
Acetyl-H3
Acetyl-H3
Input
Control
PCA^L/L

Figure 5. Upregulation of HDACs expression in Arid1a depletion islet

(A) GSEA analysis revealed the upregulation of HDAC pathway in the $PCA^{L/L}$ islets.

(B) Islets were isolated from the pancreas of the control and $PCA^{L/L}$ mice and the protein levels of HDACs were determined by Western blotting.

(C) ChIP-sequencing was performed to identify genome-wide binding of HDAC6 in control and PCAL/L mice. Distribution figure of peaks on various functional elements of genes.

(D) Differential volcano plot (Red dots represent peaks that are significantly up-regulated and blue dots represent those that are significantly down-regulated. X axis:log2 fold change of peaks. Y axis: statistical significance of the differential in log10(q-value).

(E) The most significant motif sequence. The abscissa is motif sequence. The ordinate is percentage of each base.

(F) GO enrichment histogram (X axis: number of differential peak-associated genes in this GO category. Color code is to distinguish the categories - biological processes, cellular components and molecular functions.

(G) KEGG enrichment histogram (X axis: gene number. Y axis: pathway term).

(H) Scatterplot of peak-associated genes KEGG enrichment (X axis: RichFactor. Y axis specify KEGG pathways. The size of the dot is positively correlated with the number of peak-associated genes in the pathway. Color code is to indicate Q-value ranges.

(I) Depicted are the top30 gene targets with minimum p-values identified by ChIP-Seq peak calling analysis.

(J) Genomic DNAs were collected from the control and PCAL/L islets and the binding of HDAC6 to the Arid1a-occupied region 3 (Ngn3-3) in the Ngn3 gene promoter was studied by ChIP assay. Acetylation of histone H3 around the Ngn3-3 region in the Ngn3 gene promoter was also studied by ChIP assay.

increased after Arid1a depletion in human 1.2B4 islet cells (Figure 4E). Because HDAC6 has been shown to be a repression target of Arid1a,[28] we performed chromatin immunoprecipitation-sequencing analysis (ChIP-seq) to study genome-wide HDAC6 occupancy in the control and Arid1a-depleted islet cells. Ablation of Arid1a increased the binding of HDAC6 to proximal gene promoters (<3 kb) whereas it decreased HDAC6 occupancy on 5′UTR and gene bodies (Figure 5C). Volcano plot showed 136 significantly altered genes in Arid1a-depleted islet cells (Figure 5D). The preferential binding motifs were also predicted (Figure 5E). Gene ontology analysis demonstrated the enrichment of genes in diverse biological processes (Figure 5F). Pathway analysis showed differentially expressed genes in insulin signaling, glycolysis/gluconeogenesis, and pyruvate metabolism, consisting with the diabetic phenotypes found in the $PCA^{L/L}$ mice (Figures 5G and 5H). Among the top 30 altered genes, two critical genes, *Ngn3* and *Pdx1*, involving in pancreas development and endocrine regulation were identified as HDAC6 targets (Figure 5I). ChIP assay confirmed that the binding of HDAC6 to the Arid1a-binding Ngn3-3 region in the Ngn3 promoter was enhanced and the acetylation of histone H3 (activation marks) in this region was attenuated (Figure 5J). These results suggested that Arid1a ablation increases HDAC6 expression and changes its genome-wide occupancy to impair islet development.

Therapeutic effect of HDAC inhibitor on Arid1a depletion-induced pancreas dysfunction

Vorinostat (also known as suberanilohydroxamic acid, SAHA), a clinically approved HDAC inhibitor, was given to 7-week-old $PCA^{L/L}$ mice, and blood sugar levels were continuously monitored. Treatment with SAHA did not significantly change body weight of the mice (Figure S10). However, SAHA treatment increased pancreas size, and decreased blood sugar level in the $PCA^{L/L}$ mice (Figures 6A and 6B). In addition, insulin levels in the blood and the number and size of insulin-producing islets were increased (Figures 6C and 6D). Moreover, the number of $Ngn3^{+}$ progenitor cells was upregulated (Figures 6D and 6E). Conversely, infiltration of $CD3^{+}$T cells and $F4/80^{+}$ macrophages in the pancreas was significantly decreased (Figures 6F and 6G). These data suggest that HDAC inhibitors show therapeutic benefit on Arid1a depletion-induced pancreas dysfunction by reducing immune attack of islet cells and amplifying the pool of $Ngn3^{+}$ progenitor cells.

DISCUSSION

Although the tumor-suppressive activity of Arid1a has been demonstrated in various cancers including pancreatic cancer, the functional role of Arid1a in organ development is largely unclear because conventional knockout of this gene causes embryonic lethality.[16] Recently, three studies generated pancreas-specific deletion of *Arid1a* in mice.[11–13] However, all these studies utilized Ptf1a-Cre for gene deletion. Because the expression of Ptf1a is very low in islet cells especially in β cells, Arid1a is retained in the islets of the mice, and no alteration of endocrine function has been noted. By using Pdx1-driven Cre model, we provide the first evidence that Arid1a is required for islet development.

Pdx1 is a critical transcription factor that controls the development, maturation and regeneration of β cells. Deletion of the *Pdx1* gene in β cells induces reprogramming of gene transcription, resulting in loss of β cell identify and enhancement of α cell phenotype.[29] Of interest, inactivation of *Pdx1* causes the development of DM.[29,30] However, the effects of ablation of *Arid1a* and *Pdx1* are different because pancreas-specific deletion of *Arid1a* affects

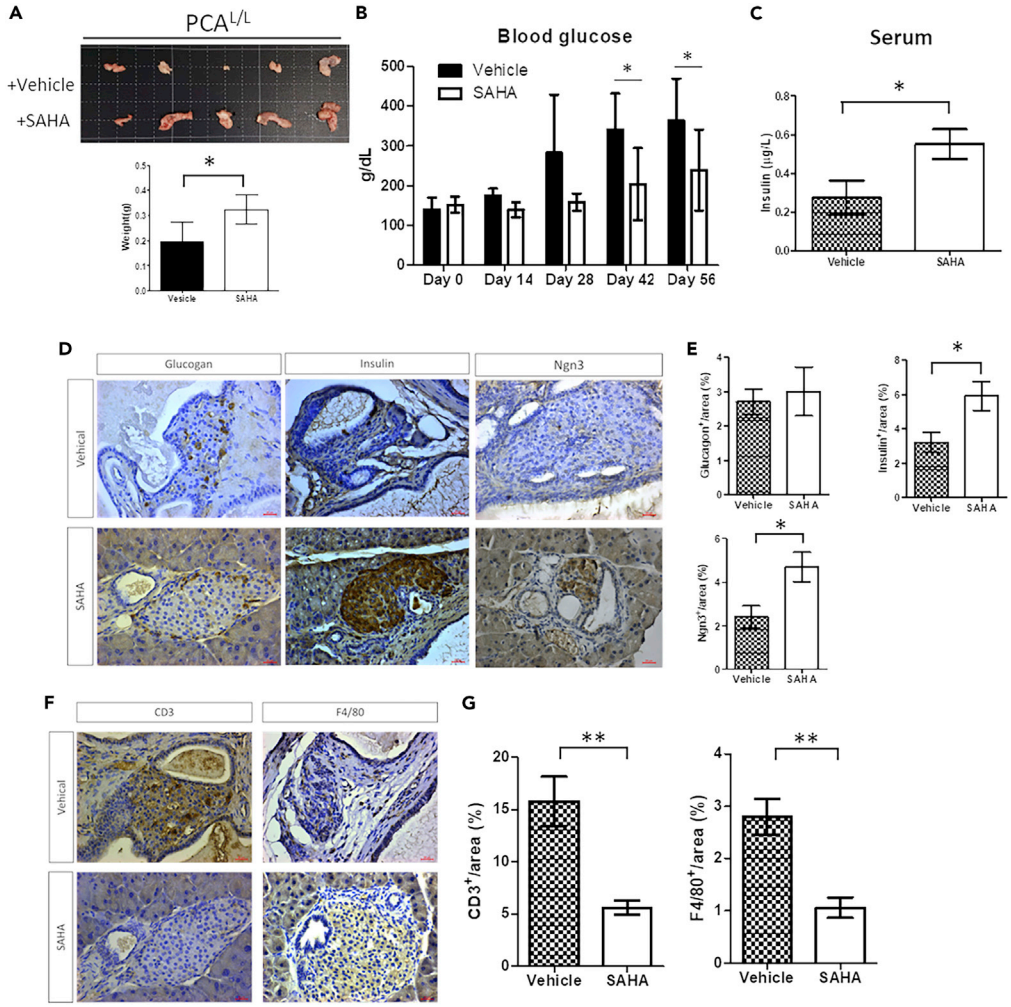

Figure 6. HDAC inhibitor suppresses the onset of DM induced by Arid1a depletion

(A) Seven-week-old PCA$^{L/L}$ mice were administered twice weekly by intraperitoneal injections of 50 mg/kg of SAHA or PBS vehicle for 4 weeks (n = 5, per group). Mice were sacrificed, and the weights of pancreases were measured. In addition, blood sugar levels were measured at different time points before animal sacrifice.

(B) Blood glucose levels in the PCA$^{L/L}$ mice treated with or without SAHA were measured every 14 days (n = 5).

(C) Blood insulin levels in the PCA$^{L/L}$ mice treated with or without SAHA were measured by ELISA assays. (n = 5).

(D) The pancreases of vehicle- or SAHA-treated PCA$^{L/L}$ mice were harvested for IHC staining to detect the expression of insulin, glucagon and neurogenin3 (Ngn3). Five independent areas were examined in a tissue slide and five tissues were counted in each group.

(E) Areas of positive insulin, glucagon and neurogenin3 immunostaining were quantified by ImageJ software.

(F) Infiltration of CD3$^+$T cells and F4/80$^+$ macrophages in the pancreas of vehicle- or SAHA-treated PCA$^{L/L}$ mice was studied by IHC staining.

(G) Areas of positive CD3$^+$ and F4/80$^+$ immunostaining were quantified by ImageJ software. *p<0.05; **p<0.01.

multiple islet cell types and reduces the expression of insulin and glucagon simultaneously, whereas ablation of *Pdx1* triggers α cell transcriptional program and glucagon production. Although Pdx1 may partially contribute to the developmental defect seen in *Arid1a*-depleted mice, it does not confer all biological effects of Arid1a in pancreas development. Our study suggests that Arid1a plays a crucial role in the regulation of pancreatic progenitor cell proliferation. One potential mediator by which Arid1a regulates the fate and maturation of islet cells is Ngn3. This transcription factor is required for endocrine lineage formation of the pancreas by controlling various downstream transcriptional factors like NeuroD1, Nkx2-2, Pax4 and Nkx6-1.[31] Our RNA sequencing data confirmed that all these transcription factors were decreased in *Arid1a*-depleted islets (Table S1). In human, development of endocrine pancreas is also dependent on Ngn3.[32] We showed that Arid1a directly binds to

the Ngn3 promoter to increase its expression and co-expression of Ngn3 and Arid1a increases insulin production in *Arid1a*-depleted islet cells. Our results suggest that Ngn3 is one of the downstream targets of Arid1a to controls pancreas development. However, other transcriptional factors like Pdx1, Hnf1b and Rfx6 (Figure 4A) may also contribute to Arid1a-mediated effect.

A complex interaction between β cells and immune cells has been implicated in the development of DM. External insults like viral infection and immune stimulators have been shown to induce local inflammation via a self-defense mechanism in the pancreas. However, whether some intrinsic mediators may promote inflammatory responses in the pancreas to promote DM pathogenesis are relatively unclear. A potential role of chromatin regulators including DNA methyltransferase, nucleosome remodeling complexes, histone acetyltransferases/deacetylases and polycomb group complex proteins have been implicated in pancreas development and DM pathogenesis.[33] However, a genetically engineered animal model to address the effect of chromatin regulators on the development and function of pancreatic islet cells is still lacking. A recent study demonstrated that embryonic deletion of the ATPase subunit Brg1 caused pancreatic hypoplasia whereas removal of another ATPase subunit Brm did not.[34] Our results showed that deletion of *Arid1a* activates interferon α signaling in the islets (Figure 2F). This cytokine has been shown to increase the expression of MHC genes in human β cells which results in enhanced immune attack and islet dysfunction.[21–23] Thus, *Arid1a* inactivation could be an intrinsic factor to modulate DM phenotype. Our hypothesis is supported by the following observations. First, bioinformatics analysis demonstrates that *ARID1A* is significantly downregulated in the pancreas or isolated islets of DM patients in independent databases (Figure S5), suggesting the phenotypic alterations found in our animal model may recapitulate at least in part of the disease progression in DM patients. Second, in addition to mutation, promoter hypermethylation of *ARID1A* gene has been reported in various human diseases.[35–37] It is possible that the decrease of ARID1A in DM patients can be induced by aberrant epigenetic regulation. Third, ARID1A reduction may contribute to β cell senescence. Recent studies demonstrated that senescence of β cells is significantly increased in the pancreas in DM patients and elimination of senescent cells improves the severity of diabetes.[38,39] Of interest, we also found the increase of cell senescence and p21 expression in Arid1a-depleted pancreas (Figures S11A and S11B).

Another important finding of this study is that pan-HDAC inhibitors show therapeutic benefit on *Arid1a* depletion-induced pancreas dysfunction. Our RNA sequencing data revealed the upregulation of HDAC pathway after *Arid1a* depletion (Figure 5A). A previous study also demonstrated that gene expressions of most of HDACs are declined during pancreas development and HDAC inhibitors may amplify endocrine progenitor pool in mice.[40] Extended from this work and our RNA sequencing data, we found that Vorinostat increases islet numbers and insulin secretion, and represses the onset of DM phenotype in *Arid1a*-depleted mice. In addition, Vorinostat also reduces inflammation and infiltration of immune cells in the islets which may prevent or attenuate immune attack and β cell death. Collectively, our study reveals the importance of Arid1a in pancreatic β cell development and in metabolic homeostasis.

Limitations of the study

We establish an animal model to study the role of Arid1a in pancreas development and reveal the importance of Arid1a in the regulation of pancreatic β cell function. However, validation of the expression of Arid1a in the pancreas of DM patients is difficult because only limited RNA sequencing and single-cell transcriptome results were available in public database. In addition, immune cell infiltration in the pancreas in *Arid1a*-depleted mice found in our study needs to be confirmed in human samples.

STAR★METHODS

Detailed methods are provided in the online version of this paper and include the following:

- KEY RESOURCES TABLE
- RESOURCE AVAILABILITY
  - Lead contact
  - Materials availability
  - Data and code availability
- EXPERIMENTAL MODEL AND SUBJECT DETAILS
  - Genetically modified mice
- METHOD DETAILS
  - Isolation of mouse pancreatic islets
  - Lentivirus production and shRNA for gene knockdown

- Transcriptomic profiling by RNA sequencing
- Chromatin immunoprecipitation (ChIP) assay
- Metabolome profiles of mice islet medium by capillary electrophoresis-time of flight (CE-TOF) analysis
- Glucose tolerance test
- Immunohistochemistry
- Western blot analysis
- Real-time-quantitative PCR analysis (RT-qPCR)
- SAHA treatment

- QUANTIFICATION AND STATISTICAL ANALYSIS

SUPPLEMENTAL INFORMATION

Supplemental information can be found online at https://doi.org/10.1016/j.isci.2022.105881.

ACKNOWLEDGMENTS

This manuscript used data acquired from the Human Pancreas Analysis Program (HPAP-RRID:SCR_016202) Database (https://hpap.pmacs.upenn.edu), a Human Islet Research Network (RRID:SCR_014393) consortium (UC4-DK-112217, U01-DK-123594, UC4-DK-112232, and U01-DK-123716). These studies were supported by the grant 110-2320-B-400-17 to W.C.H. and 109-2327-B-037-002 to L.T.C. from the Ministry of Science and Technology, Taiwan and CA-111-PP-17 to W.C.H. from the Ministry of Health and Welfare, Taiwan.

AUTHOR CONTRIBUTIONS

T.L.K. performed the experiments; T.L.K. and W.C.H. analyzed the data; K.H.C. provided the Pdx1-Cre mice; T.L.K and W.C.H. wrote and edited the manuscript. K.H.C., L.T.C., and W.C.H. conceived the project idea.

DECLARATION OF INTERESTS

The authors declare no competing interests.

Received: March 21, 2022
Revised: October 27, 2022
Accepted: December 22, 2022
Published: January 20, 2023

REFERENCES

1. Lemon, B., and Tjian, R. (2000). Orchestrated response: a symphony of transcription factors for gene control. Genes Dev. *14*, 2551–2569.
2. Cramer, P. (2019). Organization and regulation of gene transcription. Nature *573*, 45–54.
3. Hargreaves, D.C., and Crabtree, G.R. (2011). ATP-dependent chromatin remodeling: genetics, genomics and mechanisms. Cell Res. *21*, 396–420.
4. Alfert, A., Moreno, N., and Kerl, K. (2019). The BAF complex in development and disease. Epigenet. Chromatin *12*, 19.
5. Kadoch, C., and Crabtree, G.R. (2013). Reversible disruption of mSWI/SNF (BAF) complexes by the SS18-SSX oncogenic fusion in synovial sarcoma. Cell *153*, 71–85.
6. Wang, X., Haswell, J.R., and Roberts, C.W.M. (2014). Molecular pathways: SWI/SNF (BAF) complexes are frequently mutated in cancer–mechanisms and potential therapeutic insights. Clin. Cancer Res. *20*, 21–27.
7. Wu, J.N., and Roberts, C.W.M. (2013). ARID1A mutations in cancer: another epigenetic tumor suppressor? Cancer Discov. *3*, 35–43.
8. Yamamoto, S., Tsuda, H., Takano, M., Tamai, S., and Matsubara, O. (2012). Loss of ARID1A protein expression occurs as an early event in ovarian clear-cell carcinoma development and frequently coexists with PIK3CA mutations. Mod. Pathol. *25*, 615–624.
9. Yan, H.B., Wang, X.F., Zhang, Q., Tang, Z.Q., Jiang, Y.H., Fan, H.Z., Sun, Y.H., Yang, P.Y., and Liu, F. (2014). Reduced expression of the chromatin remodeling gene ARID1A enhances gastric cancer cell migration and invasion via downregulation of E-cadherin transcription. Carcinogenesis *35*, 867–876.
10. Zhu, Y.P., Sheng, L.L., Wu, J., Yang, M., Cheng, X.F., Wu, N.N., Ye, X.B., Cai, J., Wang, L., Shen, Q., and Wu, J.Q. (2018). Loss of ARID1A expression is associated with poor prognosis in patients with gastric cancer. Hum. Pathol. *78*, 28–35.
11. Kimura, Y., Fukuda, A., Ogawa, S., Maruno, T., Takada, Y., Tsuda, M., Hiramatsu, Y., Araki, O., Nagao, M., Yoshikawa, T., et al. (2018). ARID1A maintains differentiation of pancreatic ductal cells and inhibits development of pancreatic ductal adenocarcinoma in mice. Gastroenterology *155*, 194–209.e2.
12. Wang, S.C., Nassour, I., Xiao, S., Zhang, S., Luo, X., Lee, J., Li, L., Sun, X., Nguyen, L.H., Chuang, J.C., et al. (2019). SWI/SNF component ARID1A restrains pancreatic neoplasia formation. Gut *68*, 1259–1270.
13. Wang, W., Friedland, S.C., Guo, B., O'Dell, M.R., Alexander, W.B., Whitney-Miller, C.L., Agostini-Vulaj, D., Huber, A.R., Myers, J.R., Ashton, J.M., et al. (2019). ARID1A, a SWI/SNF subunit, is critical to acinar cell homeostasis and regeneration and is a barrier to transformation and epithelial-mesenchymal transition in the pancreas. Gut *68*, 1245–1258.

14. Kawaguchi, Y., Cooper, B., Gannon, M., Ray, M., MacDonald, R.J., and Wright, C.V.E. (2002). The role of the transcriptional regulator Ptf1a in converting intestinal to pancreatic progenitors. Nat. Genet. *32*, 128–134.

15. Heiser, P.W., Lau, J., Taketo, M.M., Herrera, P.L., and Hebrok, M. (2006). Stabilization of beta-catenin impacts pancreas growth. Development *133*, 2023–2032.

16. Gao, X., Tate, P., Hu, P., Tjian, R., Skarnes, W.C., and Wang, Z. (2008). ES cell pluripotency and germ-layer formation require the SWI/SNF chromatin remodeling component BAF250a. Proc. Natl. Acad. Sci. USA *105*, 6656–6661.

17. Moore, A., Wu, L., Chuang, J.C., Sun, X., Luo, X., Gopal, P., Li, L., Celen, C., Zimmer, M., and Zhu, H. (2019). Arid1a loss drives nonalcoholic steatohepatitis in mice through epigenetic dysregulation of hepatic lipogenesis and fatty acid oxidation. Hepatology *69*, 1931–1945.

18. Kaestner, K.H., Powers, A.C., Naji, A.; HPAP Consortium, and Atkinson, M.A. (2019). NIH initiative to improve understanding of the pancreas, islet, and autoimmunity in type 1 diabetes: the Human Pancreas Analysis Program (HPAP). Diabetes *68*, 1394–1402.

19. Brissova, M., Haliyur, R., Saunders, D., Shrestha, S., Dai, C., Blodgett, D.M., Bottino, R., Campbell-Thompson, M., Aramandla, R., Poffenberger, G., et al. (2018). Alpha cell function and gene expression are compromised in type 1 diabetes. Cell Rep. *22*, 2667–2676.

20. Ramos-Rodríguez, M., Raurell-Vila, H., Colli, M.L., Alvelos, M.I., Subirana-Granés, M., Juan-Mateu, J., Norris, R., Turatsinze, J.V., Nakayasu, E.S., Webb-Robertson, B.J.M., et al. (2019). The impact of proinflammatory cytokines on the beta-cell regulatory landscape provides insights into the genetics of type 1 diabetes. Nat. Genet. *51*, 1588–1595.

21. Marroqui, L., Dos Santos, R.S., Op de Beeck, A., Coomans de Brachène, A., Marselli, L., Marchetti, P., and Eizirik, D.L. (2017). Interferon-alpha mediates human beta cell HLA class I overexpression, endoplasmic reticulum stress and apoptosis, three hallmarks of early human type 1 diabetes. Diabetologia *60*, 656–667.

22. Azoury, M.E., Tarayrah, M., Afonso, G., Pais, A., Colli, M.L., Maillard, C., Lavaud, C., Alexandre-Heymann, L., Gonzalez-Duque, S., Verdier, Y., et al. (2020). Peptides derived from insulin granule proteins are targeted by CD8(+) T cells across MHC class I restrictions in humans and NOD mice. Diabetes *69*, 2678–2690.

23. Russell, M.A., Redick, S.D., Blodgett, D.M., Richardson, S.J., Leete, P., Krogvold, L., Dahl-Jørgensen, K., Bottino, R., Brissova, M., Spaeth, J.M., et al. (2019). HLA class II antigen processing and presentation pathway components demonstrated by transcriptome and protein analyses of islet beta-cells from donors with type 1 diabetes. Diabetes *68*, 988–1001.

24. Liu, X., Li, Z., Wang, Z., Liu, F., Zhang, L., Ke, J., Xu, X., Zhang, Y., Yuan, Y., Wei, T., et al. (2022). Chromatin remodeling induced by ARID1A loss in lung cancer promotes glycolysis and confers JQ1 vulnerability. Cancer Res. *82*, 791–804.

25. Qu, Y.L., Deng, C.H., Luo, Q., Shang, X.Y., Wu, J.X., Shi, Y., Wang, L., and Han, Z.G. (2019). Arid1a regulates insulin sensitivity and lipid metabolism. EBioMedicine *42*, 481–493.

26. Shibata, K. (2018). Urinary excretion of 2-Oxo Acids is greater in rats with streptozotocin-induced diabetes. J. Nutr. Sci. Vitaminol. *64*, 292–295.

27. Liu, M., Li, L., Chu, J., Zhu, B., Zhang, Q., Yin, X., Jiang, W., Dai, G., Ju, W., Wang, Z., et al. (2015). Serum N(1)-methylnicotinamide is associated with obesity and diabetes in Chinese. J. Clin. Endocrinol. Metab. *100*, 3112–3117.

28. Bitler, B.G., Wu, S., Park, P.H., Hai, Y., Aird, K.M., Wang, Y., Zhai, Y., Kossenkov, A.V., Vara-Ailor, A., Rauscher, F.J., III, et al. (2017). ARID1A-mutated ovarian cancers depend on HDAC6 activity. Nat. Cell Biol. *19*, 962–973.

29. Gao, T., McKenna, B., Li, C., Reichert, M., Nguyen, J., Singh, T., Yang, C., Pannikar, A., Doliba, N., Zhang, T., et al. (2014). Pdx1 maintains beta cell identity and function by repressing an alpha cell program. Cell Metab. *19*, 259–271.

30. Gannon, M., Ables, E.T., Crawford, L., Lowe, D., Offield, M.F., Magnuson, M.A., and Wright, C.V.E. (2008). pdx-1 function is specifically required in embryonic beta cells to generate appropriate numbers of endocrine cell types and maintain glucose homeostasis. Dev. Biol. *314*, 406–417.

31. Gradwohl, G., Dierich, A., LeMeur, M., and Guillemot, F. (2000). neurogenin3 is required for the development of the four endocrine cell lineages of the pancreas. Proc. Natl. Acad. Sci. USA *97*, 1607–1611.

32. McGrath, P.S., Watson, C.L., Ingram, C., Helmrath, M.A., and Wells, J.M. (2015). The basic helix-loop-helix transcription factor NEUROG3 is required for development of the human endocrine pancreas. Diabetes *64*, 2497–2505.

33. Campbell, S.A., and Hoffman, B.G. (2016). Chromatin regulators in pancreas development and diabetes. Trends Endocrinol. Metab. *27*, 142–152.

34. Spaeth, J.M., Liu, J.H., Peters, D., Guo, M., Osipovich, A.B., Mohammadi, F., Roy, N., Bhushan, A., Magnuson, M.A., Hebrok, M., et al. (2019). The Pdx1-bound Swi/Snf chromatin remodeling complex regulates pancreatic progenitor cell proliferation and mature islet beta-cell function. Diabetes *68*, 1806–1818.

35. Xie, H., Chen, P., Huang, H.W., Liu, L.P., and Zhao, F. (2017). Reactive oxygen species downregulate ARID1A expression via its promoter methylation during the pathogenesis of endometriosis. Eur. Rev. Med. Pharmacol. Sci. *21*, 4509–4515.

36. Luo, Q., Wu, X., Chang, W., Zhao, P., Zhu, X., Chen, H., Nan, Y., Luo, A., Zhou, X., Su, D., et al. (2020). ARID1A hypermethylation disrupts transcriptional homeostasis to promote squamous cell carcinoma progression. Cancer Res. *80*, 406–417.

37. Yoshino, J., Akiyama, Y., Shimada, S., Ogura, T., Ogawa, K., Ono, H., Mitsunori, Y., Ban, D., Kudo, A., Yamaoka, S., et al. (2020). Loss of ARID1A induces a stemness gene ALDH1A1 expression with histone acetylation in the malignant subtype of cholangiocarcinoma. Carcinogenesis *41*, 734–742.

38. Thompson, P.J., Shah, A., Ntranos, V., Van Gool, F., Atkinson, M., and Bhushan, A. (2019). Targeted elimination of senescent beta cells prevents type 1 diabetes. Cell Metab. *29*, 1045–1060.e10.

39. Aguayo-Mazzucato, C., Andle, J., Lee, T.B., Jr., Midha, A., Talemal, L., Chipashvili, V., Hollister-Lock, J., van Deursen, J., Weir, G., and Bonner-Weir, S. (2019). Acceleration of beta cell aging determines diabetes and senolysis improves disease outcomes. Cell Metab. *30*, 129–142.e4.

40. Haumaitre, C., Lenoir, O., and Scharfmann, R. (2008). Histone deacetylase inhibitors modify pancreatic cell fate determination and amplify endocrine progenitors. Mol. Cell Biol. *28*, 6373–6383.

41. Subramanian, A., Tamayo, P., Mootha, V.K., Mukherjee, S., Ebert, B.L., Gillette, M.A., et al. (2005). Gene set enrichment analysis: a knowledge-based approach for interpreting genome-wide expression profiles. Proc. Natl. Acad. Sci. U S A *102*, 15545–15550. https://doi.org/10.1073/pnas.0506580102.

42. Goto, M. (2019). [8. Image processing using ImageJ]. Nihon Hoshasen Gijutsu Gakkai Zasshi *75*, 688–692.

43. Kõressaar, T., Lepamets, M., Kaplinski, L., Raime, K., Andreson, R., and Remm, M. (2018). Primer3_masker: integrating masking of template sequence with primer design software. Bioinformatics *34*, 1937–1938.

STAR★METHODS

KEY RESOURCES TABLE

REAGENT or RESOURCE	SOURCE	IDENTIFIER
Antibodies		
Arid1a	Cell Signaling Technology	Cat# 12354; RRID:AB_2637010
Glucagon	Cell Signaling Technology	Cat# 2760; RRID:AB_659831
Insulin	Cell Signaling Technology	Cat# 3014; RRID:AB_2126503
Sox9	Abcam	Cat# ab185966; RRID:AB_2728660
CD3	Abcam	Cat# ab5690; RRID:AB_305055
Neurogenin-3	Millipore	Cat# AB5684; RRID:AB_11213023
E-Cadherin	BD Biosciences	Cat# 610182; RRID:AB_397581
Arid1a	Abcam	Cat# ab182560; RRID:AB_2313773
MafA	Santa Cruz	Cat# sc-390491; RRID:AB_2313773
GAPDH	Abcam	Cat# ab9482; RRID:AB_307272
HDAC1	Cell Signaling Technology	Cat# 5356; RRID:AB_10612242
HDAC4	Cell Signaling Technology	Cat# 5392; RRID:AB_10547753
HDAC5	Cell Signaling Technology	Cat# 2082; RRID:AB_2116626
HDAC6	Cell Signaling Technology	Cat# 7612; RRID:AB_10889735
Acetyl-Histone H3	Cell Signaling Technology	Cat# 7627; RRID:AB_10839410
Neurogenin-3	Abnova	Cat# PAB1916; RRID:AB_1577683
F4/80	Cell Signaling Technology	Cat# 70076; RRID:AB_2799771
CD31	Abcam	Cat# ab28364; RRID:AB_726362
IL1-beta	Abcam	Cat# ab8319; RRID:AB_306472
p16 INK4a	Santa Cruz	Cat# sc-468; RRID:AB_632103
p21	Santa Cruz	Cat# sc-469; RRID:AB_632121
p53	Santa Cruz	Cat# sc-126; RRID:AB_628082
Chemicals, peptides, and recombinant proteins		
SAHA	Cayman	Cat# 10009929
Lipofectamine™ 3000 Transfection Reagent	Thermo Fisher Scientific	Cat# L3000008
cOmplete™, Mini Protease Inhibitor Cocktail	Millipore Sigma	Cat# 4693124001
ProLong™ Glass Antifade Mountant with NucBlue™ Stain	Thermo Fisher Scientific	Cat# P36981
DMEM, high glucose	Thermo Fisher Scientific	Cat# 11965118
Critical commercial assays		
Mouse Insulin ELISA KIT	Mercodia	Cat# 10-1247-01
High-Capacity cDNA Reverse Transcription Kit	Thermo Fisher Scientific	Cat# 4368813
Deposited data		
Analyzed data	NCBI	GEO: GSE106148
Raw and analyzed data	This paper	GEO: GSE220638, Mendeley Data: https://data.mendeley.com/datasets/zybcfhdb58
Experimental models: Cell lines		
1.2B4	Merck Sigma	Cat# 10070103-1VL RRID:CVCL_2258

(*Continued on next page*)

Continued

REAGENT or RESOURCE	SOURCE	IDENTIFIER
Experimental models: Organisms/strains		
Arid1atm1.1Zhwa/J	The Jackson Laboratory	RRID:IMSR_JAX:027717
B6.FVB-Tg(Pdx1-cre)6Tuv/Nci	Frederick National Laboratory	RRID:IMSR_NCIMR:01XL5
Oligonucleotides		
Primers for qPCR, see Table S2	see Table S2	Primers for qPCR, see Table S2
Software and algorithms		
GraphPad Prism v9	GraphPad	RRID: SCR_00279
Living Image version 4.5	Perkin Elme	https://www.perkinelmer.com/product/spectrum-200-living-image-v4series-1-128113
GSEA	Subramanian et al.[41]	https://www.gsea-msigdb.org/gsea/index.jsp
ImageJ	Goto,[42]	https://imagej.nih.gov/ij/index.html
Primer3	Koressaar et al.[43]	http://primer3.ut.ee/

RESOURCE AVAILABILITY

Lead contact

Further information and requests for resources and reagents should be directed to and will be fulfilled by the lead contact, Wen-Chun Hung (hung1228@nhri.org.tw).

Materials availability

This study did not generate new unique reagents.

Data and code availability

- Next-generation sequencing data generated in this study have been deposited in the NCBI GEO with accession number GSE220638. Metabolism data, ChIP-seq data and RNA-seq data reported in this paper have been deposited at Mendeley Data and are publicly available with accession number https://data.mendeley.com/datasets/zybcfhdb58.
- This paper does not report original code.
- Any additional information required to reanalyze the data reported in this paper is available from the lead contact upon request.

EXPERIMENTAL MODEL AND SUBJECT DETAILS

Genetically modified mice

Pdx-1Cre and *Arid1a*$^{tm1.1Zhwa}$ mice were obtained from the Mouse Models of Human Cancers Consortium (MMHCC) and The Jackson Laboratory under material transfer agreements. Mice were genotyped as described by the MMHCC and The Jackson Laboratory (JAX) PCR protocols for strains 01XL5 and strain *Arid1a*$^{tm1.1Zhwa}$. Experiments were performed on off-spring male mice (4 weeks-old) derived from homozygous mating. The age of mice used in this study is from 4-weeks-old (for drug treatment) to 1-year-old (for medium survival determination). Animal studies were approved by the Institutional Animal Care and Use Committee of the National Health Research Institutes.

METHOD DETAILS

Isolation of mouse pancreatic islets

To isolate mouse islets, pancreases were perfused through the common bile duct with a Hanks' balanced salt buffer (HBSS)-collagenase solution (1.4 g/L; collagenase type 4) and digested in the same solution in a 37°C water bath for 26–28 min. After shaking for 15 seconds, pancreases were washed three times with HBSS supplemented with 0.5% bovine serum albumin (BSA) and filtrated through 500 μm and 70 μm cell strainers (Corning). Islets were retained in the 70 μm cell strainer while the cell mixture passing through the 70 μm cell strainer containing the exocrine stoma were discarded. Islets were collected and pooled

into a Petri dish with RPMI-1640 (GIBCO) containing 11.1 mM glucose, 100 units/ml penicillin, 100 μg/mL streptomycin, 2 mM Glutamax, 50 μg/mL gentamycin, 10 μg/mL Fungison and 10% fetal calf serum (Invitrogen). Islets were used directly for RNA isolation or overexpression of Ngn3 and Arid1a cultured in a humid environment containing 5% CO_2 for transfection assay.

Lentivirus production and shRNA for gene knockdown

The plasmids required for shRNA lentivirus production were purchased from the National RNAi Core Facility (Academia Sinica, Taiwan). The pLKO.1-shRNA vectors used for knockdown of ARID1A were TRCN0000059090 and TRCN0000059091 (Human), TRCN0000071396 and TRCN0000071397 (Mouse). The pLKO.1-emptyT control plasmid was TRCN0000208001. To generate recombinant lentivirus, 293T cells were co-transfected with package plasmid (pCMV8.91), envelop VSV-G plasmid (pMD.G), and shRNA expressing construct. The virus-containing supernatant was harvested at 48 h after transfection. For infection, NIT-1 cells were incubated with the virus-containing medium supplemented with 8 μg/mL of polybrene and the infected cells were selected by 2 μg/mL of puromycin for 72 h before harvesting for western blot analysis.

Transcriptomic profiling by RNA sequencing

RNAs were isolated from islet tissues using Trizol extraction followed by purification with the Qiagen RNAeasy kit. Quantity and purity of RNAs were assessed at 260 nm and 280 nm using a Nanodrop (ND-1000; Labtech International). Three hundred ng of each sample was amplified and labeled using the GeneChip WT Sense Target Labeling and Control Reagents (900652) for expression analysis. Hybridization was performed against the Affymetrix GeneChip MoGene 1.0 ST array. The arrays were hybridized at 45°C for 17 hat 60 rpm. The arrays were washed and stained with streptavidin-phycoerythrin (GeneChip® Hybridization, Wash, and Stain Kit, 900720). The signal intensities on the arrays were scanned using Affymetrix GeneChip® Scanner 3000. The results were analyzed using Expression Console software (Affymetrix) and Transcriptome Analysis Console software (Affymetrix) with default RMA parameters. Differential expressed genes (DEGs) were defined as the genes with a 2.0-fold change and p value <0.05. The DEG lists were uploaded from a Microsoft Excel spreadsheet onto Metacore 6.13 software (GeneGo pathways analysis) (http://www.genego.com). Pathway analyses of DEGs were also performed using GSEA (www.gsea-msigdb.org) and KEGG (www.genome.jp/kegg).

Chromatin immunoprecipitation (ChIP) assay

ChIP assays with the anti-Arid1a antibody (Abnova, MAB15809) were performed using the EZ-ChIP Kit (Merck Millipore) according to the manufacturer's instruction. Cellular lysates were subjected to five sets of sonication on wet ice with a 60 Sonic Dismembrator (Fisher Scientifi c). Each set consisted of 8 seconds of sonication separated by 1-minute intervals on ice and sonicated to an average DNA length between 300 and 700 bp. Chromatin concentrations were determined using a BCA protein assay kit (Pierce). Chromatin samples were diluted to 300 μg per 200 μL of nuclear lysis buffer and then cleared by centrifugation at 10,000g. Precleared chromatin samples (200 μL each) were added to 800 μL (1:5 dilution) of ChIP dilution buffer (50 mM Tris-Cl (pH 7.5); 150 mM NaCl; 5 mM EDTA; 0.5% IGEPAL CA-630; 1% TX-100) and incubated with 10 μg of prebound ARID1A Protein G beads (Invitrogen) overnight at 4°C. The Protein G bead-anti-ARID1A immune conjugates were washed twice with 1 mL ChIP dilution buffer, three times with 1 mL ChIP dilution buffer supplemented with 500 mM NaCl, twice with 1 mL ChIP dilution buffer, followed by a final wash in 1 mL low-salt TE buffer (10 mM Tris-Cl (pH 8.0); 1 mM EDTA; 50 mM NaCl). The immunoprecipitated samples were eluted in 100 μL of elution buffer (50 mM NaHCO3; 1% SDS) at 62 °C for 20 min. using an Eppendorf tube mixer. The crosslinks were reversed by adding NaCl to a final concentration of 0.2 M followed by an overnight incubation at 65 C. The samples were then deproteinated with Proteinase K and purified using the ChIP DNA Clean & Concentrator kit (Zymo Research) according to the manufacturer's Instructions. Precipitated DNA was analyzed using PCR primers for *Ngn3* promoter listed in Table S2. Real-time quantitative PCR using Ssofast PCR master mix (Biorad) and a IQ5 thermocycler (Biorad).

Metabolome profiles of mice islet medium by capillary electrophoresis-time of flight (CE-TOF) analysis

The conditioned medium of islets isolated from control and Arid1a-depleted mice were used for metabolome analysis. Samples (80 μL) were mixed with 20 μL of Milli-Q water containing internal standards.

Metabolome analysis was performed by Basic Scan package of Human Metabolome Technologies (HMT) using CE-TOF (HMT, Tokyo, Japan). Hierarchical cluster analysis (HCA) and principal component analysis (PCA) were performed by statistical analysis software (HMT). The profiles of peaks with putative metabolites were presented on metabolic pathway maps using VANTED (Visualization and Analysis of Networks containing Experimental Data) software.

Glucose tolerance test

Thirteen-week-old mice (n = 5) were fasted for 16 h in the morning and intraperitoneally injected with 2 g/kg of glucose. Blood glucose levels were continuously measured for 15, 30, 60, and 120 min using a glucometer (Accu-Chek; Roche Diagnostics). In addition, blood samples were collected at the indicated time points for later plasma insulin determination by using an insulin ELISA kit (Mercodia, Uppsala, Sweden) following manufacturer's protocol.

Immunohistochemistry

Pancreatic specimens were fixed with 10% buffered formalin, dehydrated in ethanol, embedded with paraffin, and stained with hematoxylin and eosin. Standard procedures for IHC analysis were performed according to manufacturer's protocol. Deparaffinize and rehydrate formalin-fixed paraffin-embedded tissue section. Add enough drops of Hydrogen Peroxide Block to cover the sections. Apply Protein Block and incubate for 5 minutes at room temperature to block nonspecific background staining. Apply primary antibody and incubate according to manufacturer's protocol. Apply Biotinylated goat anti rabbit IgG(H+L) and incubate for 10 minutes at room temperature. Apply Streptavidin Peroxidase and incubate for 10 minutes at room temperature. Add 20ul DAB Chromogen to 1 mL of DAB Substrate, mix by swirling and apply to tissue. Add enough drops of Hematoxylin to cover the section. Rinse 7–8 times in tap water. Add Mounting Medium to cover the section. The image of the IHC stained slides were captured using a Carl Zeiss Axioskop 2 plus microscope (Carl Zeiss, Thornwood, NY). The following primary antibodies were used: Anti-glucagon (Cell Signaling Technology, Cat# 2760); Anti-cytokeratin 19 (GeneTex, GTX112666); Anti-insulin (Cell Signaling Technology, Cat# 3014); Anti-ARID1A (Abnova, MAB15809); Anti-IL-1β (Abcam, ab9722); Anti-F4/80 (Cell Signaling Technology, Cat# 70076).

Western blot analysis

For Western blot analysis, cells were harvested by RIPA lysis buffer (150 mmol/L NaCl, 10 mmol/L Tris, pH 7.5, 1% NP40, 1% deoxycholate, 0.1% SDS, protease inhibitor cocktail). Cellular proteins were resolved by the 10% Bis-Tris gradient gel (Invitrogen), transferred to the polyvinylidene difluoride membrane, blocked in 5% non-fat milk in PBS/Tween-20, and probed by the following primary antibodies: anti-insulin (Cell Signaling Technology, Cat# 3014); anti-ARID1A (Abnova, MAB15809); anti-Neurogenin3 (Santa Cruz Biotechnology, sc-374442), and anti-MafA (Santa Cruz Biotechnology, sc-390491). Chemiluminescence substrate was applied using SuperSignal West Pico Chemiluminescent Substrate (#34080, Thermo Fisher Scientific) or SuperSignal West Femto Maximum Sensitivity Substrate (#34095, Thermo Fisher Scientific) and blots were analyzed using the ChemiDoc Touch Imaging System (#1708370, Bio-Rad).

Real-time-quantitative PCR analysis (RT-qPCR)

Total RNAs were extracted from tissues and cells using TRIzol reagents (Invitrogen, USA) according to the manufacturer's protocol and quantified by Nanodrop (Thermo Fisher Scientific, USA). Synthesis of cDNAs was executed using the GoScript RT system (Promega). Quantitative PCR was done as previously described [18]. The qRT-PCR analysis was performed using PowerTrack SYBR Green Master Mix (Applied Biosystems) on an IQ5 RT-PCR system (BioRad, USA). 18S or GAPDH was used as the internal control to normalize the data to determine the relative expression of the target genes by using the $2-\Delta\Delta Ct$ method. The primers for RT-qPCR were listed in Table S2.

SAHA treatment

For *in vivo* treatment, SAHA was first dissolved in DMSO at a dose of 50 mg/mL, which was then diluted with phosphate-buffered saline to a final concentration of 5 mg/mL directly before use. Seven-week-old $PCA^{L/L}$mice were administered twice weekly by intraperitoneal injections of 50 mg/kg of SAHA or phosphate-buffered saline vehicle for 4 weeks (n = 5, per group). Blood sugar levels were continuously monitored every two weeks for 8 weeks. At the end of the experiment, blood samples were collected and insulin

levels were quantified by ELISA kit. Mice were sacrificed, and the pancreases were collected for histological analyses.

QUANTIFICATION AND STATISTICAL ANALYSIS

All experiments were performed at least in triplicate, and representative data were shown. Statistical analysis was performed by one- or two-way ANOVA using Prism 5.0 software to identify differences among different experimental groups. The median survival was estimated using the Kaplan-Meier method. Quantitative data were expressed as mean ± SEM and p value less than 0.05 was considered significant. The significance was presented as *, $p < 0.05$; **, $p < 0.01$; ***, $p < 0.001$; and no significant difference was presented as ns.